Title

Stokes parameters imaging of light reflected from biological tissue using polarization-sensitive optical coherence tomography

Authors

de Boer, Johannes F
Milner, Thomas E
Nelson, J Stuart

Publication Date

1999-04-30

DOI

10.1117/12.347482

Stokes parameters imaging of light reflected from biological tissue using Polarization Sensitive Optical Coherence Tomography

Johannes F. de Boer[a], Thomas E. Milner[b], and J. Stuart Nelson[a]

[a]Beckman Laser Institute and Medical Clinic, University of California, Irvine, 1002 Health Sciences Road East, Irvine, California 92612, USA

[b]Biomedical Engineering Program, University of Texas, Austin, TX 78712

ABSTRACT

Polarization sensitive optical coherence tomography (PS-OCT) was used to determine the depth resolved Stokes parameters of light backscattered from highly scattering biological samples. Through simultaneous detection of the amplitude and relative phase of signal fringes in orthogonal polarization states formed by interference of light backscattered from turbid media and a mirror in the reference arm of a Michelson interferometer, changes in the Stokes parameters due to the optical phase delay between light propagating along the fast and slow axes of birefringent media were measured. Inasmuch as fibrous structures in many biological tissues influence the polarization state of light backscattered, PS-OCT is a potentially useful technique to image the structural properties of turbid biological materials. The method can also be applied to the investigation of birefringent properties in highly scattering materials such as ceramics and crystals.

Keywords: Optical Coherence Tomography, Birefringence, Stokes parameters, Imaging

1. INTRODUCTION

First reported in the field of fiber optics,[1-3] optical coherence tomography (OCT) has become an important high resolution technique for biomedical imaging. OCT utilizes a Michelson interferometer with a broadband source with high spatial coherence to measure light backscattered from turbid media with high spatial resolution ($\sim 10\ \mu m$) and sensitivity (>100 dB).[4] In general, OCT images display the depth resolved magnitude of backscattered light. Except for an early study by Hee *et al.*,[5] the polarized nature of light was not considered until recently when depth resolved birefringence images of bovine tendon[6,7] and myocardium[8] were reported. In this letter we present an analysis to determine the depth resolved Stokes parameters of light backscattered from turbid media using polarization sensitive optical coherence tomography (PS-OCT). Compared to previous methods, where only the fringe intensity in two orthogonal polarization states was used in the signal analysis,[6-8] the present work incorporates the phase relationship between interference fringes in each polarization channel to characterize completely the polarization state. Analysis of depth resolved changes in the Stokes parameters of light backscattered from the sample provides a means to determine spatial variations in sample birefringence and corresponding structural properties.

2. EXPERIMENTAL SET-UP

Figure 1 shows a schematic of the PS-OCT system used in our experiments. Light from a superluminescent diode ($0.8\ mW$, $\lambda_0 = 856\ nm$ and spectral FWHM $\Delta\lambda = 25\ nm$) was linearly polarized. A quarter wave plate (QWP) positioned in the reference path produced linearly polarized light at 45^0 with respect to the vertical after double passage. The intensity noise was reduced by a factor of 50 by placing a neutral density filter in the reference path.[9] A second QWP in the sample path produced circularly polarized light that was focused (f=50 mm) to a spot size of 17μm diameter on the sample. After double passage through the QWP, light in the sample arm was in an arbitrary (elliptical) polarization state, determined by the sample birefringence. After recombination in the detection path, the light was split into horizontal and vertical components by a polarizing beamsplitter (PBS) and focused (f=50 mm) on 25 μm diameter pinholes placed directly in front of the detectors to detect a single spatial mode. Two dimensional images were formed by lateral movement of the sample at 1 mm/s (x-direction), repeated after each

Corresponding author: JFdB, Email: deboer@bli.uci.edu; Telephone: 949-824-3284; Fax: 949-824-8413

Part of the SPIE Conference on Coherence Domain Optical Methods in Biomedical Science and Clinical Applications III • San Jose, California • January 1999
SPIE Vol. 3598 • 0277-786X/99/$10.00

10 μm incremental longitudinal displacement (z-direction). Active beam focus tracking in the tissue ($n = 1.4$) was achieved by translating the PZT retroreflector assembly after each transverse scan.[10] The interference fringe carrier frequency ($\sim$ 6 kHz) was generated by modulating the optical path length of the reference arm over 20 μm with a 50 Hz triangular waveform. An image pixel was calculated using the interference signal recorded over the central 10 μm of the 20 μm reference arm modulation. Transverse and longitudinal pixel dimensions in the images were 10 μm by 10 μm.

3. THEORY

An expression for the depth resolved Stokes parameters of light backscattered from a turbid birefringent sample was derived in terms of the measured amplitude and relative phase of the interference fringes in orthogonal polarization states.[11] In our analysis, the electric fields are represented in their complex analytic form,[12] $E(z) = \int \tilde{e}(k) \exp(-ikz)dk$, with $k = 2\pi/\lambda$ and $\tilde{e}(k) = 0$ if $k < 0$. From the Wiener-Khinchine theorem, it follows $\langle \tilde{e}^*(k)\tilde{e}(k')\rangle = S(k)\delta(k-k')$, which defines $\tilde{e}(k)$ in terms of the spectral density $S(k)$ of the source, and angular brackets denote ensemble averaging. Since light from the reference arm was split equally into the horizontal and vertical polarization states, the electric field in the reference arm is given by

$$E_{x,y}(z_r) = \int_{-\infty}^{\infty} \tilde{e}(k) \exp(-2ikz_r)dk \tag{1}$$

with z_r the length of the reference arm. The electric field in the sample arm is given by,

$$\vec{E}(z_s) = \int_{-\infty}^{\infty} \sqrt{R(z_s)}\vec{a}(k, z_s)\tilde{e}(k) \exp(-2ikz_s)dk \tag{2}$$

where $\sqrt{R(z_s)}$ describes the reflectivity at depth z_s and the attenuation of the coherent beam by scattering, and $\vec{a}(k, z_s)$ characterizes the polarization state of light backscattered from depth z_s, with $\vec{a}^*(k, z_s)\cdot\vec{a}(k, z_s) = 1$. Following the definitions in Mandel and Wolf[13] the Stokes parameters s_j with $j = 0, 1, 2, 3$ of the electric field $\vec{E}(z_s)$ are

$$s_j(z_s) = \mathrm{tr}[\boldsymbol{\sigma}_j \mathbf{J}] = R(z_s) \int [\vec{a}^*(k, z_s)\boldsymbol{\sigma}_j\vec{a}(k, z_s)]S(k)dk \tag{3}$$

with $\mathbf{J}$ the 2×2 coherency matrix,[13] $J_{k,l} = \langle E_k^* E_l\rangle$ where k, l each take on the values x and y, $\boldsymbol{\sigma}_0$ the 2×2 identity matrix and $\boldsymbol{\sigma}_1$, $\boldsymbol{\sigma}_2$ and $\boldsymbol{\sigma}_3$ the Pauli spin matrices. The interference fringe intensity between light in the sample and reference paths is given by

$$\vec{\mathcal{I}}(z_s, \Delta z) = 2\mathrm{Re}\begin{pmatrix} \langle E_x^*(z_r)E_x(z_s)\rangle \\ \langle E_y^*(z_r)E_y(z_s)\rangle \end{pmatrix} = \sqrt{R(z_s)} \int 2\mathrm{Re}[\vec{a}(k, z_s) \exp(-2ik\Delta z)]S(k)dk \tag{4}$$

with $\Delta z = z_s - z_r$. The Fourier transform of $\vec{\mathcal{I}}(z_s, \Delta z)$ with respect to Δz is

$$\vec{\tilde{\mathcal{I}}}(z_s, 2k) = \frac{1}{2\pi}\sqrt{R(z_s)}\vec{a}(k, z_s)S(k). \tag{5}$$

Using Eq. 5 the Stokes parameters in Eq. 3 can be expressed in terms of $\vec{\tilde{\mathcal{I}}}(z_s, 2k)$,

$$s_j = (2\pi)^2 \int [\vec{\tilde{\mathcal{I}}}^*(z_s, 2k)\boldsymbol{\sigma}_j\vec{\tilde{\mathcal{I}}}(z_s, 2k)]/S(k)dk. \tag{6}$$

Signals $\mathcal{I}_x(z_s, \Delta z)$ and $\mathcal{I}_y(z_s, \Delta z)$ were digitized at 5×10^4 points per second each, with z_s the average reference arm length at reference arm modulation Δz. For each image pixel, the Fourier transform of the central 10 μm (256 points) of the reference arm modulation was taken and digitally bandpass filtered between 5 - 7 kHz. The Stokes parameters for each pixel were calculated according to Eq. 6, with the spectral density $S(k)$ estimated by $|\tilde{\mathcal{I}}(z_s, 2k)| = 1/(2\pi)\sqrt{R(z_s)}S(k)$. To determine the polarization state of light backscattered from the sample, the Stokes vector is multiplied by the inverse of the Mueller matrix associated with the QWP in the sample arm, $s_0 \mapsto s_0$, $s_1 \mapsto -s_3$, $s_2 \mapsto s_2$ and $s_3 \mapsto s_1$. Because the spectral density $S(k)$ is estimated by $|\tilde{\mathcal{I}}(z_s, 2k)|$ in Eq. 6, $s_0(z_s)$ is related to the backscattered intensity summed over both polarization channels by $\langle|\vec{\mathcal{I}}(z_s)|\rangle \propto \sqrt{R(z_s)}s_0(z_s)$. s_1 and s_2 characterize linear polarization in frames rotated by 45^0 with respect to each other, the signs of s_1 and s_2 indicate predominant linear polarization in either of two orthogonal planes, while s_3 describes circular polarization, the sign of s_3 denoting the handedness. The Stokes parameters satisfy the relationship $s_0^2 \geq s_1^2 + s_2^2 + s_3^2$, and a parameter $P = \sqrt{s_1^2 + s_2^2 + s_3^2}/s_0$ ranges from 1 to 0 and indicates the degree of polarization.

4. RESULTS

OCT images of the Stokes parameters were formed by grayscale coding $20 \log s_0(z_s)$ from 0 to -48 dB, where the 0 dB level corresponded to the maximum signal in an image, and by grayscale coding the polarization state parameters s_1, s_2 and s_3 normalized on the intensity s_0 from 1 to -1, and P from 1 to 0. Contour lines indicating $1/3$ and $-1/3$ fractions of the normalized parameters s_1, s_2 and s_3 were calculated after low pass filtering by convolving the images with a Gaussian filter of 4×4 pixels and overlaid with the original image. Figures 2 and 3 show the four Stokes parameters, measured in *ex vivo* rat skeletal muscle and bone, respectively. In our experimental configuration, the image of the Stokes parameter s_3 is similar to that obtained by grayscale coding the birefringence induced phase retardation, $\phi = \arctan \sqrt{\mathcal{I}_x^2(z)/\mathcal{I}_y^2(z)} = k_0 z \delta$, as was done previously,[5,7,8] with the exact relationship being $s_3/s_0 = \cos 2\phi$.

The birefringence in Figure 2 is attributed to the high structural order (anisotropy) of skeletal muscle fibers. Several periods of s_1, s_2 and s_3, cycling back and forth between 1 and -1, are observed. The birefringence δ was determined by measuring the distance of a full s_3 period, which corresponds to a phase retardation of $\pi = k_0 z \delta$, giving $\delta = 2.4 \times 10^{-3}$. The greater birefringence in skeletal muscle as compared to the myocardium reported by Everett *et al.*[8] is attributed to structural differences. In myocardium, the fibers are oriented in different directions, and not necessarily parallel to the tissue surface. The skeletal muscle imaged in Figure 2 shows a high degree of muscle fiber alignment, the orientation of which can be determined by finding the rotation of the reference frame that minimizes the variance in either s_1 or s_2. Our analysis of this image gives an angle of -7^0 with respect to the vertical of one of the optic axes, consistent with a fiber direction that was almost perpendicular to the horizontal scan direction.

In Figure 3 an interesting feature in a portion of the s_3 parameter image of *ex-vivo* rodent bone is the apparent loss of birefringence. However, the s_1 parameter image reveals that the predominant orientation of the linear polarization in either of two orthogonal planes is reversed around the region showing the apparent loss of birefringence. The region indicating birefringence loss (s_3-image) may represent a transition of the dominant orientation of the optic axis.

5. DISCUSSION

Determination of the depth resolved Stokes parameters of light backscattered from turbid birefringent media using PS-OCT reveals structural information that can not be determined by previous methods[5–8] that only analyzed the intensity in two orthogonal polarization channels. In a sample wherethe optical axes were constant, the birefringence and axes orientations were determined. A future analysis of the evolution of the Stokes parameters will allow depth resolved determination of the birefringence and changes in the orientation of the optical axes in turbid birefringent media. Also of interest for future study is the parameter P that may reveal information on the presence of multiply scattered light in OCT images through a decrease in the degree of polarization.

ACKNOWLEDGMENTS

Research grants from the Institutes of Arthritis, Musculoskeletal and Skin Diseases and Heart, Lung and Blood, and the National Center for Research Resources at the National Institutes of Health, U.S. Department of Energy, Office of Naval Research and the Beckman Laser Institute Endowment are gratefully acknowledged.

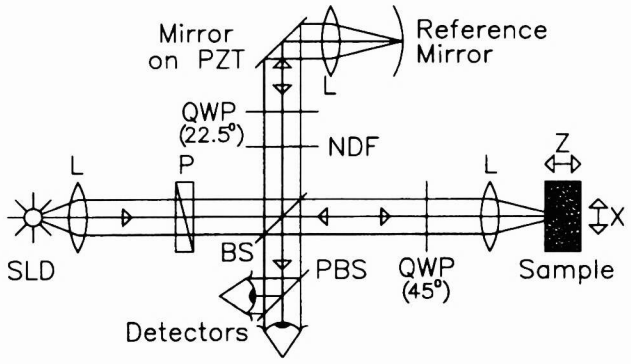

Figure 1. Schematic of the PS-OCT system. SLD: superluminescent diode, L: lens, P: polarizer, BS: beam splitter, QWP: quarter wave plate, NDF: neutral density filter, PBS: polarizing beam splitter. The mirror on a piezo electric transducer (PZT) modulates the reference arm length over 20 μm to generate the carrier frequency. The PZT retroreflector assembly is mounted on a translation stage to allow for active focus tracking in the sample. Two dimensional images were formed by lateral movement of the sample at constant velocity (x-direction), repeated after each longitudinal displacement (z-direction).

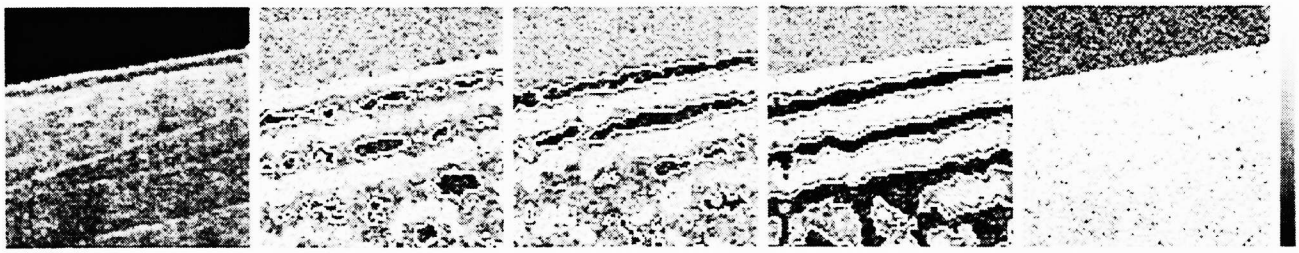

Figure 2. PS-OCT images of *ex vivo* rat muscle, 1 $mm \times 1$ mm, pixel size 10 $\mu m \times 10$ μm. From left to right, the Stokes parameters s_0, s_1, s_2, s_3 and degree of polarization P. The gray scale to the right gives the magnitude of signals, ranging from 0 to -48 dB for s_0, from 1 to -1 for s_1, s_2 and s_3, and from 1 to 0 for P. White lines in images s_1, s_2 and s_3 are contours at 1/3 (white to gray transition) and $-1/3$ (gray to black transition) signal levels, respectively.

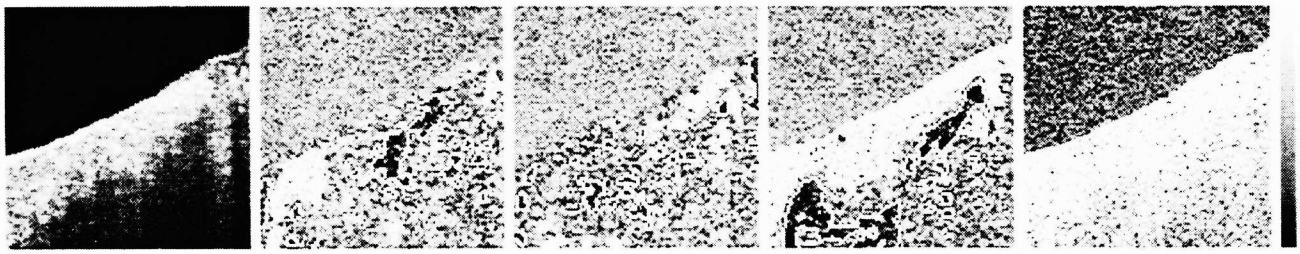

Figure 3. PS-OCT images of *ex vivo* rat bone, 1 $mm \times 1$ mm, pixel size 10 $\mu m \times 10$ μm. From left to right, the Stokes parameters s_0, s_1, s_2 and s_3, and degree of polarization P. The gray scale to the right gives the magnitude of signals, ranging from 0 to -48 dB for s_0, from 1 to -1 for s_1, s_2 and s_3, and from 1 to 0 for P. White lines in images s_1, s_2 and s_3 are contours at 1/3 (white to gray transition) and $-1/3$ (gray to black transition) signal levels, respectively.

REFERENCES

1. R. C. Youngquist, S. Carr, and D. E. N. Davies, "Optical coherence-domain reflectometry: a new optical evaluation technique," *Appl. Opt.* **12**, pp. 158–160, 1987.
2. K. Takada, I. Yokohama, K. Chida, and J. Noda, "New measurement system for fault location in optical waveguide devices based on an interferometric technique," *Appl. Opt.* **26**, pp. 1603–1606, 1987.
3. B. L. Danielson and C. D. Whittenberg, "Guided-wave reflectometry with micrometer resolution," *Appl. Opt.* **26**, p. 2836, 1987.
4. D. Huang, E. A. Swanson, C. P. Lin, J. S. Schuman, W. G. Stinson, W. Chang, M. R. Hee, T. Flotte, K. Gregory, C. A. Puliafito, and J. G. Fujimoto, "Optical coherence tomography," *Science* **254**, pp. 1178–1181, Nov. 1991.
5. M. R. Hee, D. Huang, E. A. Swanson, and J. G. Fujimoto, "Polarization-sensitive low-coherence reflectometer for birefringence characterization and ranging," *J. Opt. Soc. Am. B* **9**, pp. 903–908, June 1992.
6. J. F. de Boer, T. E. Milner, M. J. C. van Gemert, and J. S. Nelson, "Two-dimensional birefringence imaging in biological tissue using polarization sensitive optical coherence tomography," *Opt. Lett.* **22**, pp. 934–936, June 1997.
7. J. F. de Boer, T. E. Milner, M. J. C. van Gemert, and J. S. Nelson, "Two-dimensional birefringence imaging in biological tissue using polarization-sensitive optical coherence tomography," *Proc. Soc. Photo-Opt. Instrum. Eng.* **3196**, pp. 32–37, 1998.
8. M. J. Everett, K. Schoenenberger, B. W. Colston Jr., and L. B. Da Silva, "Birefringence characterization of biological tissue by use of optical coherence tomography," *Opt. Lett.* **23**, pp. 228–230, Feb. 1998.
9. W. V. Sorin and D. M. Baney, "A simple intensity noise reduction technique for optical low-coherence reflectometry," *IEEE Photonics Tech. Lett.* **4**, pp. 1404–1406, Dec. 1992.
10. Z. Chen, T. E. Milner, D. Dave, and J. S. Nelson, "Optical doppler tomographic imaging of fluid flow velocity in highly scattering media," *Opt. Lett.* **22**(64), p. 64, 1997.
11. J. F. de Boer, T. E. Milner, and J. S. Nelson, "Determination of the depth resolved stokes parameters of light backscattered from turbid media using polarization sensitive optical coherence tomography," *Opt. Lett.* **5**, pp. 300–302, 1999.
12. L. Mandel and E. Wolf, *Optical Coherence and Quantum Optics*, ch. 3. Cambridge University Press, Cambridge, England, 1995.
13. L. Mandel and E. Wolf, *Optical Coherence and Quantum Optics*, ch. 6. Cambridge University Press, Cambridge, England, 1995.